Neutral Gas Sympathetic Cooling of an Ion in a Paul Trap

Kuang Chen, Scott T. Sullivan, and Eric R. Hudson
Department of Physics and Astronomy, University of California, Los Angeles, California 90095, USA
(Received 15 October 2013; published 11 April 2014)

A single ion immersed in a neutral buffer gas is studied. An analytical model is developed that gives a complete description of the dynamics and steady-state properties of the ions. An extension of this model, using techniques employed in the mathematics of economics and finance, is used to explain the recent observation of non-Maxwellian statistics for these systems. Taken together, these results offer an explanation of the long-standing issues associated with sympathetic cooling of an ion by a neutral buffer gas.

DOI: 10.1103/PhysRevLett.112.143009 PACS numbers: 37.10.Ty, 05.40.-a

The fact that two isolated objects in thermal contact tend to the same temperature is the most basic tenet of thermodynamics. It is also the essence of the technique of sympathetic cooling, where a sample is prepared at a desired temperature by bringing it into thermal contact with a much larger body already at the desired temperature. It is difficult to overstate the importance of this technique as it underpins applications ranging from basic refrigeration to quantum information science.

It may be considered surprising then that a gas of ions trapped in a radio-frequency (rf) Paul trap and immersed in a reservoir of neutral atoms does not equilibrate to the same temperature as the neutral atoms. Instead, the ions are found to have a higher temperature than the neutral gas, and in some cases are heated so much that they escape the trap. Since the early work of Major and Dehmelt [1] it has been known that this apparent contradiction with the laws of thermodynamics is due to the fact that ions are subject to a time-dependent confining potential and are therefore not an isolated system. However, despite pioneering work by Dehmelt and others [2,3], an accurate analytical description of the relaxation process has not yet been achieved. Given the recent surge in interest in hybrid atom-ion systems [4–14], where ions are immersed in baths of ultracold atoms, there is currently a strong need for such a description so that these systems can be understood and optimized.

Building upon the important work of Moriwaki *et al.* [2], here we present a simple kinematic model, which accurately describes the ion relaxation process. This model, which has been verified by detailed molecular dynamics simulations, provides a simple and accurate means to calculate both the relaxation dynamics and the properties of the ion steady state. This model also provides significant physical intuition for the problem and, as such suggests several ways for optimizing ongoing and planned experiments in fields as diverse as quantum chemistry [4–13], mass spectrometry [15], and quantum information [16].

In the remainder of this work, we first review the basics of ion trapping and introduce the time-averaged ion kinetic energy. We then consider the effect of a collision with a neutral particle on the evolution of the kinetic energy of a single ion in a Paul trap and show that due to the presence of the time-dependent potential the collision center-of-mass frame energy is not conserved. Following this result, we develop a rate equation model, which accounts for the relaxation and exchange of the ion energy in all three dimensions. We then present simple formulas for the calculation of the ion temperature relaxation rate and steady-state value, as well as the dependency of these values on the ion trapping parameters and particle masses. We establish the validity of these results by comparing them to a detailed molecular dynamics simulation. We conclude with an explanation for the recent observation [17] of non-Maxwellian distribution functions for these systems.

Ion trap dynamics.—The trajectory, r_j, and velocity, v_j, of an ion (mass m_i and charge e) in a linear Paul trap (field radius r_0, rf trapping voltage V_{rf}, rf frequency Ω, dc endcap voltage U_{ec}, axial length $2z_0$, and geometrical factor κ) can be expanded as a linear superposition of two orthogonal Mathieu functions $c(a_j, q_j; \tau)$ and $s(a_j, q_j; \tau)$ with coefficients A_j and B_j,

$$\begin{bmatrix} r_j(\tau) \\ v_j(\tau) \end{bmatrix} = \begin{bmatrix} c_j(\tau) & s_j(\tau) \\ \dot{c}_j(\tau) & \dot{s}_j(\tau) \end{bmatrix} \begin{bmatrix} A_j \\ B_j \end{bmatrix}, \tag{1}$$

where $j = x,\ y,\ z$, $\tau = \Omega t/2$ and the dependence on the Mathieu parameters $(\{a_x, a_y, a_z\} = \{-a, -a, 2a\}$ and $\{q_x, q_y, q_z\} = \{q, -q, 0\}$ with $q = 4eV_{rf}/m_i r_0^2\Omega^2$ and $a = 4\ \kappa eU_{ec}/m_i z_0^2\Omega^2)$ is suppressed [1]. The Fourier transform of $c_j(\tau)$ and $s_j(\tau)$ is a discrete spectrum,

$$c_j(\tau) + \imath s_j(\tau) = \sum_{n=-\infty}^{\infty} C_{2n} e^{\imath(\beta_j + 2n)\tau}. \tag{2}$$

The $n = 0$ term corresponds to the "typical" motion of a harmonic oscillator—i.e., the secular ion motion. The remaining terms with $n \neq 0$ represent the components of the ion motion driven by the rf field—i.e., the so-called micromotion.

 © 2014 American Physical Society

As a result of this spectrum, the instantaneous kinetic energy is not a conserved quantity. Instead, energy coherently flows back and forth between the kinetic energy of the ion and the confining electric field at frequency $n\Omega$. Therefore, it is useful to define the time-averaged kinetic energy

$$W_j = \frac{m}{2}\lim_{T\to\infty}\frac{1}{2T}\int_{-T}^{T} v_j^2 d\tau = \frac{m}{2}\overline{\dot{c}_j^2}(A_j^2 + B_j^2), \quad (3)$$

where the bar denotes the time average. Inverting Eq. (1), W_j is related to the instantaneous coordinates r_j and v_j through

$$W_j = \frac{m\overline{\dot{c}_j^2}}{2w_{0,j}^2}\Big((\dot{c}_j^2 + \dot{s}_j^2)r_j^2 + (c_j^2 + s_j^2)v_j^2 - 2(c_j\dot{c}_j + s_j\dot{s}_j)r_j v_j\Big), \quad (4)$$

where $w_{0,j}$ is the Wronskian of c_j and s_j. W_j includes contributions from both the random thermal motion of the ion, i.e., the secular energy, and the micromotion. The ratio of the secular energy U_j to the total average kinetic energy is simply

$$\eta_j \equiv \frac{U_j}{W_j} = \frac{|C_0|^2}{\sum_{n=-\infty}^{\infty}|C_{2n}|^2}. \quad (5)$$

In the x and y directions, the micromotion energy is given by $W_{mm,j} = W_j - U_j$ and for $q < 0.4$, $\eta_{x,y} \approx 1/2$. In the z direction where the trapping field is time independent ($q = 0$), $c_z(\tau)$ and $s_z(\tau)$ simply become the cosine and sine functions. Thus, all micromotion sidebands vanish and $\eta_z = 1$.

Modeling the collision process.—When a trapped ion is immersed in a buffer gas of neutral atoms of mass m_n and density ρ, the Mathieu trajectory of the ion is modified by interactions with the neutral atoms. The ion-neutral interaction potential is comprised of a long-range attraction $V(r) = -C_4/2r^4$ and short-range repulsion, where C_4 is given by $C_4 = \alpha_p e^2/(4\pi\epsilon_0)^2$, and α_p is the polarizability of the neutral atom. Recent work [18], has explored the effects of this potential at ultracold temperatures, showing that the perturbations of the ion trajectory by the C_4 potential can lead to heating of the ion. Here we do not consider this effect, but given that the characteristic length of the C_4 interaction [19] is small compared to the trap dimension we treat the collision as a pointlike interaction. As will be seen, this approximation is justified, despite the important result of Ref. [18], as the effects considered here typically lead to temperatures that preclude the observation of the effects considered in Ref. [18]. We also make the additional simplifying assumptions that the density of the neutral atoms is constant and that inelastic processes, such as charge exchange, do not occur.

Because the motion of the ion differs significantly in the radial and axial directions of a linear Paul trap, the relaxation and redistribution of energy is significantly more complicated than in a time-independent harmonic trap [20]. We therefore describe the statistically averaged evolution of the ion kinetic energy $\mathbf{W} = [W_x, W_y, W_z]^{\mathrm{T}}$ by a three-dimensional rate equation,

$$\frac{d\langle\mathbf{W}(t)\rangle}{dt} = -\Gamma\mathbf{M}(\langle\mathbf{W}(t)\rangle - \mathbf{W}_{\mathrm{st}}), \quad (6)$$

where Γ is an average collision rate (which may depend on energy), $\mathbf{M}$ is a 3×3 "relaxation matrix" that accounts for energy damping and redistribution among the three trap directions, and $\mathbf{W}_{\mathrm{st}}$ is the steady-state kinetic energy. The angled bracket denotes averaging of the sympathetic cooling experiment over multiple trials.

In order to calculate both Γ and $\mathbf{M}$ it is necessary to know the neutral-ion differential elastic scattering cross section $d\sigma_{el}/d\Omega$, which, given an interaction potential, is a straightforward quantum scattering calculation [21]. Regardless of the specific atom-ion potential, however, several generic arguments can be made. First, the differential cross section always exhibits a large forward scattering peak at all energy scales [22]. Thus, the majority of atom-ion collisions lead to only slightly deflected trajectories, resulting in a very small change in $\mathbf{W}$. Therefore, as originally argued by Dalgarno and co-workers [23], to prevent an overestimate of the energy redistribution due to collisions the momentum transfer (diffusion) differential cross section, i.e., $(d\sigma_d/d\Omega) = (1-\cos\theta)d\sigma_{el}/d\Omega$ should be used to calculate the total atom-ion collision rate, where θ is the angle of scattering. Second (and fortuitously), the diffusion differential cross section is approximately isotropic in scattering angle, especially after thermal averaging, and agrees quite well with the simple Langevin cross section [24] $\sigma_d \approx \sigma_L = \pi\sqrt{2C_4/E}$—see [25] sect. A, for a comparison of a quantum scattering calculation to the Langevin differential cross section. Therefore, we replace the cross section by an isotropic profile which integrates to σ_L. Under this approximation, the average collision rate $\Gamma = 2\ \pi\rho\sqrt{C_4/\mu}$ (where μ is the reduced mass) becomes energy independent and the calculation of $\mathbf{M}$ is greatly simplified. As demonstrated below, the validity of this approximation is confirmed by comparison to a detailed molecular dynamics simulation, which uses the full quantum differential cross section. The resulting error in the relaxation rate is smaller than 25% for collision energies down to 1 mK.

With the collision rate in hand, the relaxation matrix $\mathbf{M}$ is calculated by considering the kinematics of a collision between an ion and neutral atom as follows. Suppose that at time τ an ion undergoes an elastic collision with an incoming neutral atom of velocity $\mathbf{v}_n$. Conservation of momentum and energy for the collision dictates that the velocity of the ion after the collision with the neutral atom is given by the sum of center-of-mass velocity and the scattered relative velocity [26],

$$\mathbf{v}' = \frac{1}{1+\tilde{m}}\mathbf{v} + \frac{\tilde{m}}{1+\tilde{m}}\mathbf{v}_n + \frac{\tilde{m}}{1+\tilde{m}}\mathcal{R}(\mathbf{v}-\mathbf{v}_n), \quad (7)$$

where $\tilde{m} = m_n/m_i$ is the mass ratio and $\mathcal{R}$ is the collision rotation matrix, which, following the above discussion, is isotropic. Likewise, because the characteristic length of the C_4 interaction [19] is small compared to the trap dimension, the position of the ion is assumed to be unchanged during the collision, i.e., $\mathbf{r}' = \mathbf{r}$. By requiring that $\mathbf{r}'$ and $\mathbf{v}'$ also correspond to a Mathieu solution through Eq. (1), a new set of oscillation amplitude (A_j', B_j') and, thus, the average kinetic energy after the collision $\mathbf{W}'$, can be found.

This last step is the critical difference between sympathetic cooling in static and time-dependent traps, which is illustrated with the following one-dimensional example. In a static trap, like that in Ref. [27], if a collision happens at position $x = a$ that reduces the velocity such that $v_x' = 0$, a trapped particle of mass m begins a "new" oscillation trajectory, $x' = a\cos(2\pi\sqrt{k/m}t)$, where k is the trap spring constant. This collision always reduces the total energy of the particle. By contrast, in the time-dependent potential of a linear Paul trap, because of the terms in Eq. (2) with $n \neq 0$, it is possible that even though the collision brings the particle to rest, the particle may have a *higher* energy after the collision. This can be seen by again considering a collision that leads to $v_x' = 0$, which, depending on the rf phase, could be accomplished by having large and opposite contributions to the velocity from the $n = 0$ (secular) mode and $n \neq 0$ (micromotion) modes. Thus, even though the particle is momentarily stopped, it could leave the collision on a trajectory of higher amplitude.

With this prescription, the calculation of $\mathbf{M}$ is straightforward. Using Eq. (7) with Eq. (4), and taking the average with respect to $\mathbf{v_n}$, $\mathcal{R}$ and τ, the average change of $\mathbf{W}$ per collision is found by $\langle\mathbf{W}'\rangle - \langle\mathbf{W}\rangle = -\mathbf{M}\langle\mathbf{W}\rangle + \mathbf{N}$ (see [25] sect. B), where

$$\mathbf{M} = -\frac{\tilde{m}}{(1+\tilde{m})^2}\left(\mathbf{I} - \tilde{m}\begin{bmatrix} \frac{2\epsilon-1}{3} & \frac{\alpha}{6} & \frac{\alpha}{6} \\ \frac{\alpha}{6} & \frac{2\epsilon-1}{3} & \frac{\alpha}{6} \\ \frac{1}{6} & \frac{1}{6} & -\frac{1}{3} \end{bmatrix}\right) \tag{8}$$

and

$$\mathbf{N} = \frac{\tilde{m}}{(1+\tilde{m})^2}\begin{bmatrix} \alpha\langle W_n\rangle \\ \alpha\langle W_n\rangle \\ \langle W_n\rangle \end{bmatrix}. \tag{9}$$

The components of the steady-state kinetic energy $\mathbf{W}_{\rm st} = -\mathbf{M}^{-1}\mathbf{N}$ reduce to

$$\frac{W_{{\rm st},x}}{\langle W_n\rangle} = \frac{W_{{\rm st},y}}{\langle W_n\rangle} = \frac{9(2+\tilde{m})\alpha}{18-3\tilde{m}(\alpha+4\epsilon-4)-2\tilde{m}^2(\alpha+2\epsilon-1)}$$
$$\frac{W_{{\rm st},z}}{\langle W_n\rangle} = \frac{3[6+\tilde{m}(2+\alpha-4\epsilon)]}{18-3\tilde{m}(\alpha+4\epsilon-4)-2\tilde{m}^2(\alpha+2\epsilon-1)}, \tag{10}$$

where $\langle W_n\rangle$ is the average kinetic energy of the neutral atom in each dimension, and α and ϵ are defined by integrals of Mathieu functions (see [25] sect. B), and for low values of q and a, their numerical values are approximated by [28],

$$\alpha \approx 2 + 2q^{2.24}, \quad \epsilon \approx 1 + 2.4q^{2.4}.$$

Model results.—First, shown in Fig. 1(a) are the components of $\mathbf{W}_{\rm st}$ normalized by $\langle W_n\rangle$ obtained from Eq. (10). Also, shown in this figure are the results of a detailed molecular dynamics simulation, described in [25], sect. C. In the limit of a light neutral atom ($\tilde{m} \approx 0$) and $q \to 0$, $\alpha \approx 2$, $\mathbf{W}_{\rm st}/\langle W_n\rangle \approx [2, 2, 1]^{\rm T}$. Thus, at steady state,

$$\langle U_x\rangle = \langle U_y\rangle = \langle U_z\rangle = \langle W_{mm,x}\rangle = \langle W_{mm,y}\rangle = \langle W_n\rangle,$$

a result often referred to as the "equipartition" [29] of kinetic energy between secular motion and micromotion. As $\tilde{m}$ increases, the steady-state secular energy deviates from equipartition and becomes much higher than $\langle W_n\rangle$. As q increases, this deviation becomes significant more quickly.

Second, the solution to Eq. (6) is a linear combination of three fundamental relaxation processes, whose rates are determined by the three eigenvalues of $\mathbf{M}$. The asymptotic behavior of the energy evolution is governed by the slowest relaxation rate, $\Gamma\lambda_0$, where λ_0, the smallest eigenvalue of $\mathbf{M}$, is

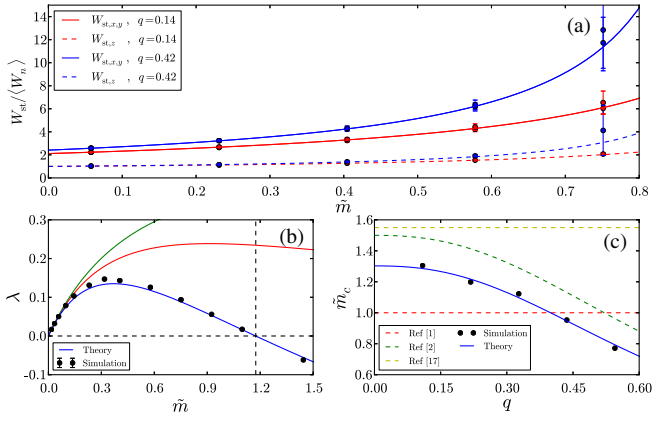

FIG. 1 (color online). (a) $\mathbf{W}_{\rm st}$ as a function of $\tilde{m}$ for $q = 0.14$ (red) and $q = 0.42$ (blue). The axial and radial components of $\mathbf{W}_{\rm st}$ are denoted by dashed and solid lines (theory) and dots (simulation). (b) Eigenvalues of $\mathbf{M}$ as a function of $\tilde{m}$ for fixed $q = 0.14$ and $a = 0$. Black dots are asymptotic relaxation rates (normalized by Γ) from numerical simulations. Lines are three calculated eigenvalues of $\mathbf{M}$. The smallest one (blue line) intersects $\lambda = 0$ line at $\tilde{m} = \tilde{m}_c$, which separates cooling from heating. (c) Simulated (dots) and calculated (blue line) critical mass ratio $\tilde{m}_c$ as a function of trap q parameter, as compared to previous results in Refs. [1,2,17].

$$\lambda_0 = \frac{\tilde{m}}{(1+\tilde{m})^2}\left(1-\frac{\tilde{m}}{\tilde{m}_c}\right), \tag{11}$$

and $\tilde{m}_c$ is the critical mass ratio given in terms of trap parameters as,

$$\tilde{m}_c = \frac{3[4-\alpha-4\epsilon+\sqrt{\alpha^2+8\alpha(1+\epsilon)+16\epsilon^2}]}{4(2\epsilon+\alpha-1)}. \tag{12}$$

The eigenvalues of $\mathbf{M}$ are shown in Fig. 1(b) and are compared to the asymptotic relaxation rates observed in the simulation. For $\tilde{m} \ll \tilde{m}_c$, the cooling rate from Eq. (11) is similar to the traditional sympathetic cooling result up to a numerical factor [20]. In this regime, the initial positive slope of λ results from enhanced energy transfer efficiency through collisions with neutral atoms of similar mass. However, the additional factor $1-(\tilde{m}/\tilde{m}_c)$ causes λ to reach a maximum and decrease to negative values once $\tilde{m}$ exceeds $\tilde{m}_c$. At this point, it is observed in the simulation that the oscillation amplitude of the ion grows with collisions, until the ion becomes too energetic to be trapped, regardless of the energy of the buffer gas.

The transition from sympathetic cooling to heating by a buffer gas is thus defined by $\tilde{m} = \tilde{m}_c$ and is shown in Fig. 1(c) as a function of q along with the results of the molecular dynamics simulations and previous results from other models of the process [1,2,17]. Taken together the results of Figs. 1(a)–1(c), make the case for using as small a buffer gas mass and as low q as possible, if significant sympathetic cooling is desired.

Non-Maxwellian statistics in an ion trap.—As originally observed in the seminal work of DeVoe [17], the peculiarity of sympathetic cooling in an ion trap is also manifested in the steady-state energy distribution of the ion, which features a heavy power-law tail due to the random amplifications of the ion energy by collisions. To gain a quantitative understanding of how this distribution arises, consider a simplified model, in which the motion of the ion and neutral atom are restricted to one dimension, and $\mathcal{R} = -1$ in Eq. (7). In (A, B) space, collisions result in a random walk given by

$$\begin{bmatrix} A_{N+1} \\ B_{N+1} \end{bmatrix} = \left(\mathbf{I} + \frac{\zeta}{w_0}\begin{bmatrix} s\dot{c} & s\dot{s} \\ -c\dot{c} & c\dot{s} \end{bmatrix}_{\tau_N}\right)\begin{bmatrix} A_N \\ B_N \end{bmatrix} + \frac{\zeta v_n}{w_0}\begin{bmatrix} s \\ c \end{bmatrix}_{\tau_N}, \tag{13}$$

where $\zeta = 2\tilde{m}/(1+\tilde{m})$, $[A_{N+1}, B_{N+1}]^{\mathrm{T}}$ are the coordinates after the Nth collision, which occurs at $\tau = \tau_N$ ($N = 1, 2, \ldots, \infty$). The τ_N constitute an array of Poissonian variables, with average interval equal to Γ^{-1}. As can be seen from Eq. (13), the random walk in (A, B) space has both additive and multiplicative terms. As is well known in the statistics of economics and finance [30], multiplicative terms in the random walk give rise to the power-law distribution as follows.

A recurrence relation for W_N can be derived from Eqs. (3) and (13), and if only the distribution of high energy ions, i.e., $W_N \gg \langle W_n \rangle$ is considered, this relation reduces to $W_{N+1} = CW_N$, where the multiplicative coefficient C is given by

$$C(\tau_N, \theta_N) = 1 + 2\zeta \frac{s\dot{c}}{w_0}\bigg|_{\tau_N-\theta_N} + \frac{\zeta^2}{w_0^2}(c^2+s^2)|_{\tau_N}\dot{c}^2|_{\tau_N-\theta_N}, \tag{14}$$

and $\tan\theta_N = B_N/A_N$. Because W only depends on A^2+B^2, it is expected that as $N \to \infty$, θ_N becomes uniformly distributed in the range of $[0, 2\pi)$ and uncorrelated with τ_N. $Q(C)$, the probability density of C, is calculated from Eq. (14) and exhibits random amplification of the ion energy, i.e., $C > 1$, as shown in Fig. 2 panels (a) and (c) for different values of $\tilde{m}$ and q.

Because of this random amplification, W develops a power-law tail in its probability density at steady state, i.e., $P(W) \propto W^{-(\nu+1)}$, where ν can be found numerically from the condition $\langle C^\nu \rangle = 1$ [31]. Figure 2, panels (b) and (d), compare the prediction to the energy distribution extracted from a molecular dynamics simulation, which subjects the ion to 10^6 trials, in each of which the ion undergoes 10^4 collisions, for each $\tilde{m}$ and q parameter. As $\tilde{m}$ and q increase random amplification becomes more likely, causing the energy distribution to become more non-Maxwellian. In comparison, there is no such random amplification from collisions in a static trap (see [25] sect. D for details).

By considering the value of ν as $\tilde{m} \to 0$ and $\tilde{m} \to \infty$, we find that the power can be approximated as $\nu_{1D} \approx 1.67/\tilde{m} - 0.67$ in one dimension (see [25] sect. E). To extend the above discussion to a full 3D model, C necessarily becomes a 3×3 stochastic matrix, and the theory of stochastic matrix products [32], which is beyond the current scope, must be considered. Nonetheless, one expects $\zeta_{3D} \approx (1/2)\zeta_{1D}$ because in three dimensions $\mathcal{R}$ average to zero, thus,

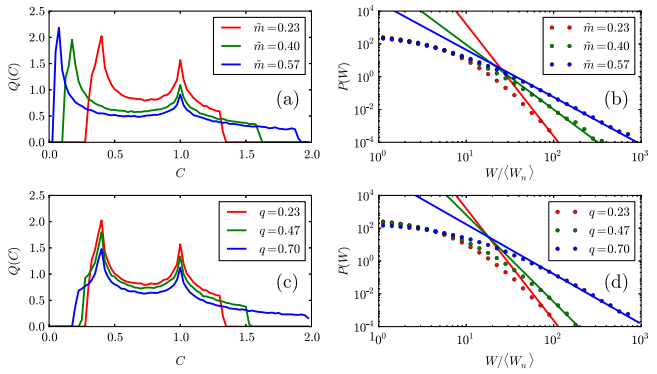

FIG. 2 (color online). Probability density of the multiplicative noise $Q(C)$ and corresponding ion's energy $P(W)$ for the 1D model from simulations for fixed $q = 0.23$ [lines in panel (a) and (b)], and fixed $\tilde{m} = 0.23$ [dots in panel (c) and (d)]. The tail of $P(W)$ is fitted to the power-law form of $W^{-(\nu+1)}$ [solid line in panel (c) and (d)], where ν is given by $\langle C^\nu \rangle = 1$.

$\nu_{3D} \approx 2\nu_{1D}$, which agrees reasonably well with the empirically extracted power law of DeVoe, $\nu_{emp} \approx 4/\tilde{m} - 1$.

In summary, we have developed an analytical model that accurately predicts the steady-state value and dynamics of the kinetic energy of a single ion immersed in a neutral buffer gas. The transition from sympathetic cooling to heating, and its dependence on trap parameters and masses of the particles have also been explained. Finally, we have confirmed that the recent observation of non-Maxwellian statistics [17] for a trapped ion can be attributed to random heating collisions and provided a means to approximate the expected power law of the energy distribution. Taken together, these results solve the longstanding issues and questions that have existed since Dehmelt first considered this problem over forty years ago. We believe that these results will be critical for the design and interpretation of experiments in the rapidly growing field of hybrid atom-ion physics [4–13].

We thank John Bollinger for guiding discussions. This work was supported by the ARO Grant No. W911NF-10-1-0505 and NSF Grant No. PHY-1005453.

[1] F. Major and H. Dehmelt, Phys. Rev. **170**, 91 (1968).
[2] Y. Moriwaki, M. Tachikawa, Y. Maeno, and T. Shimizu, Jpn. J. Appl. Phys. **31**, L1640 (1992).
[3] F. Vedel, J. André, M. Vedel, and G. Brincourt, Phys. Rev. A **27**, 2321 (1983).
[4] A. T. Grier, M. Cetina, F. Oručević, and V. Vuletić, Phys. Rev. Lett. **102**, 223201 (2009).
[5] C. Zipkes, S. Palzer, C. Sias, and M. Köhl, Nature (London) **464**, 388 (2010).
[6] C. Zipkes, S. Palzer, L. Ratschbacher, C. Sias, and M. Köhl, Phys. Rev. Lett. **105**, 133201 (2010).
[7] F. H. J. Hall, M. Aymar, N. Bouloufa-Maafa, O. Dulieu, and S. Willitsch, Phys. Rev. Lett. **107**, 243202 (2011).
[8] W. G. Rellergert, S. T. Sullivan, S. Kotochigova, A. Petrov, K. Chen, S. J. Schowalter, and E. R. Hudson, Phys. Rev. Lett. **107**, 243201 (2011).
[9] W. G. Rellergert, S. T. Sullivan, S. J. Schowalter, S. Kotochigova, K. Chen, and E. R. Hudson, Nature (London) **495**, 490 (2013).
[10] S. T. Sullivan, W. G. Rellergert, S. Kotochigova, and E. R. Hudson, Phys. Rev. Lett. **109**, 223002 (2012).
[11] S. Schmid, A. Härter, and J. H. Denschlag, Phys. Rev. Lett. **105**, 133202 (2010).
[12] L. Ratschbacher, C. Zipkes, C. Sias, and M. Köhl, Nat. Phys. **8**, 649 (2012).
[13] L. Ratschbacher, C. Sias, L. Carcagni, J. Silver, C. Zipkes, and M. Köhl, Phys. Rev. Lett. **110**, 160402 (2013).
[14] D. S. Goodman, I. Sivarajah, J. E. Wells, F. A. Narducci, and W. W. Smith, Phys. Rev. A **86**, 033408 (2012).
[15] M. Drewsen, A. Mortensen, R. Martinussen, P. Staanum, and J. L. Sørensen, Phys. Rev. Lett. **93**, 243201 (2004).
[16] E. R. Hudson, Phys. Rev. A **79**, 032716 (2009).
[17] R. DeVoe, Phys. Rev. Lett. **102**, 063001 (2009).
[18] M. Cetina, A. T. Grier, and V. Vuletić, Phys. Rev. Lett. **109**, 253201 (2012).
[19] B. Gao, Phys. Rev. Lett. **104**, 213201 (2010).
[20] R. deCarvalho, J. M. Doyle, B. Friedrich, T. Guillet, J. Kim, D. Patterson, and J. D. Weinstein, Eur. Phys. J. D **7**, 289 (1999).
[21] H. Friedrich, *Theoretical Atomic Physics* (Springer Verlag, New York, 2005).
[22] P. Zhang, A. Dalgarno, and R. Côté, Phys. Rev. A **80**, 030703 (2009).
[23] A. Dalgarno, M. R. C. McDowell, and A. Williams, Phil. Trans. R. Soc. A **250**, 411 (1958).
[24] P. Langevin, Ann. Chim. Phys. **5**, 245 (1905).
[25] See Supplemental Material at http://link.aps.org/supplemental/10.1103/PhysRevLett.112.143009, which includes Refs. [33–35].
[26] C. Zipkes, L. Ratschbacher, C. Sias, and M. Köhl, New J. Phys. **13**, 053020 (2011).
[27] W. C. Campbell, E. Tsikata, H.-I. Lu, L. D. van Buuren, and J. M. Doyle, Phys. Rev. Lett. **98**, 213001 (2007).
[28] K. Chen, S. T. Sullivan, W. G. Rellergert, and E. R. Hudson, Phys. Rev. Lett. **110**, 173003 (2013).
[29] T. Baba, and I. Waki, Appl. Phys. B: Lasers Opt. **74**, 375 (2002).
[30] X. Gabaix, Annual Review of Economics **1**, 255 (2009).
[31] H. Takayasu, A. H. Sato, and M. Takayasu, Phys. Rev. Lett. **79**, 966 (1997).
[32] H. Kesten, Acta Math. **131**, 207 (1973).
[33] B. R. Johnson, J. Chem. Phys. **67**, 4086 (1999).
[34] M. Abramowitz and I. A. Stegun, *Handbook of Mathematical Functions with Formulas, Graphs, and Mathematical Tables* (Dover Publications, New York, 1964).
[35] T. Matthey, T. Cickovski, S. Hampton, A. Ko, Q. Ma, M. Nyerges, T. Raeder, T. Slabach, and J. A. Izaguirre, ACM Trans. Math. Softw. **30**, 237 (2004).